Ho‘oponopono: A Radar Calibration CubeSat

Larry K. Martin, Nicholas G. Fisher, Windell H. Jones, John G. Furumo, James R. Ah Heong Jr.,
Monica M. L. Umeda, Wayne A. Shiroma
University of Hawaii
2540 Dole Street, Honolulu, HI 96822; 808-956-7218
larrymar@hawaii.edu

ABSTRACT

To accurately identify and track objects over its territories, the US military must regularly monitor and calibrate its 80+ C-band radar tracking stations distributed around the world. Unfortunately, only two calibration satellites are currently in service, and both have been operating well past their operational lifetimes. Losing either satellite will result in a community of users that no longer has a reliable means of radar performance monitoring and calibration. This paper not only presents the first radar calibration satellite in a CubeSat form factor, but also demonstrates the ability of a university student team to address an urgent operational need at very low cost while simultaneously providing immense educational value. Our CubeSat is named Ho‘oponopono (“to make right” in Hawaiian), an appropriate name for a calibration satellite. The government-furnished payload suite consists of a C-band transponder, GPS unit, and associated antennas, all housed in a 3U CubeSat form factor. Ho‘oponopono was the basis for the University of Hawaii’s participation in the AFOSR University Nanosat-6 Program, a rigorous two-year satellite design and fabrication competition. Ho‘oponopono was also selected by NASA as a participant in its CubeSat Launch Initiative for an upcoming launch.

MISSION OVERVIEW

Accurately tracking objects of interest over US territories using radar has been and will continue to be an important issue related to national security. As in any high-precision instrument, verifying a radar station’s ability to accurately track objects requires a calibration process.

Although radar calibration methods have existed for many years, satellite calibration has numerous advantages over these other methods. A boresight tower, for example, lacks the dynamic characteristics of an orbiting satellite, making it an unrealistic target. Aircraft targets, while dynamic, are limited in calibrating multiple radar stations simultaneously. Multipath problems are essentially eliminated with satellites due to their high elevation angles as well.

Since 1969, there have been five different Radar Performance Monitoring (RPM) satellites: GEOS-B, GEOS-C, GEOSAT, Radar Calibration (RADCAL), and DMSP F-15[1-2]. RADCAL was the first satellite dedicated to RPM and launched from a Scout rocket in 1993 with the primary mission of providing calibration data for numerous Department of Defense C-band radar systems distributed around the world[3]. To carry out these calibrations, RADCAL carries two C-band transponders, a dual-frequency Doppler beacon transmitting at 150 and 400 MHz, and a tracking, telemetry, and control unit. In an effort to standardize the procedures required to make use of a GPS-based system as a backup orbital determination system, two Trimble TANS Quadrex, non-military GPS receivers were also put onboard as a secondary, experimental payload.

Commissioned under a one-year contract-to-launch schedule, RADCAL is currently operating over 15 years past its expected lifetime and has had higher power degradations over the years, making it more evident that a replacement system will soon be needed[4]. DMSP-15, launched in 1999, is operating eight years beyond its expected lifetime.

In total, 13 tri-service agencies, NASA, and international major range organizations located in 23 geographic locations supporting 109 radars and 80+ user programs are supported by RADCAL and DMSP F-15[5]. This high volume of users, coupled with the likelihood of the current RADCAL satellite failing any day, further motivates the need of a replacement system.

The Joint Space Operations Center, for example, is a RADCAL beneficiary whose calibration needs are crucial given that its Space Situational Awareness Operations Cell maintains space data and performs satellite screenings for all man-made objects orbiting Earth to mitigate satellite collisions[6-7].

This paper presents the first RADCAL solution packaged in a CubeSat form factor (Figure 1), designed entirely by a team of students at the University of Hawaii (UH). Appropriately named for its calibration mission, Ho'oponopono ("to make right" in the Hawaiian language) is currently in the final stages of development for launch to address an imminent operational need.

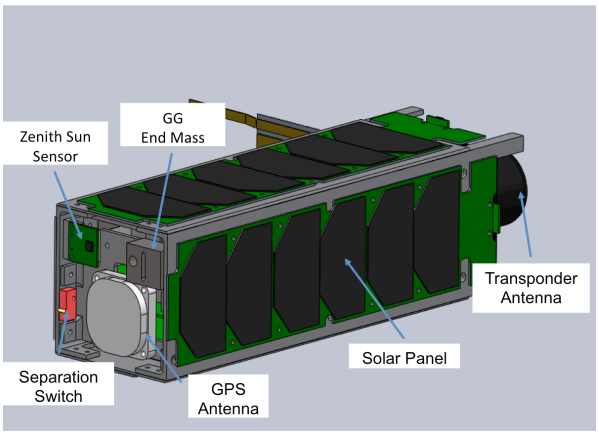

Figure 1: CAD Drawing of Ho'oponopono CubeSat

TRANSPONDER-BASED TRACKING

Conventional skin radar methods using pulse and continuous (i.e., Doppler) tracking have been employed for decades. While Ho'oponopono can be used for skin tracking, it is also capable of transponder-based radar tracking as well.

A transponder-based radar system works as follows: after being interrogated by the appropriate radar signal sequence, the on-board transponder sends back a regenerated, amplified version of the received signal, essentially acting as a microwave repeater[8]. A non-coherent transponder entails a frequency shift in the response signal, while a coherent transponder entails no frequency shift[9]. Compared to skin radar, a transponder-based system has the advantage of operating as a point-tracking source.

Another advantage of using transponder-based radar tracking is higher received power. The power returned to a skin-tracking radar is given by

$$P(returned) = \frac{P_t G^2 \lambda^2 \sigma}{(4\pi)^3 R^4} \quad (1)$$

where P_t = transmitted power; G = radar station antenna gain; σ = radar cross section of target; λ = wavelength of transmitted pulse; and R = distance between radar station and target[10]. It is assumed in (1) that a monostatic radar system is used, i.e., the same radar station is both transmitting and receiving; if a bistatic radar system were used, i.e., if the receiving station is located elsewhere, (1) will differ slightly.

The output power required from a transponder, on the other hand, is given by

$$P(transponder) = \frac{P_0 G_t A_r g}{4\pi R^2} \quad (2)$$

where P_0 = peak transmitting power of radar station; G_t = transponder antenna gain; A_r = effective aperture (area) of radar station antenna; g = gain of transponder amplifier; and R = distance between radar station and transponder[11].

Comparing (1) and (2), it is clear that for a given distance R, a weaker signal will be received using skin tracking radar. It should also be noted that transponders can have large output power values, e.g., the ~170 W for Ho'oponopono's transponder.

Another unique transponder characteristic is code spacing, a security and identification mechanism designed to restrict and limit interrogation responses to intended users. This is implemented by configuring the transponder to respond to a specific signal sequence, e.g., a pulse signal of predetermined length repeated twice in a given time interval. This same methodology is used in aircraft transponders, which operate in several different modes, depending on the received signal's code spacing[12].

Consider a transponder configured to respond to the interrogation signal shown in Figure 2, for example. In this scenario, the transponder responds if and only if the two pulse signals are 0.8 μs long and 2.0 μs apart, and ignores all other interrogations.

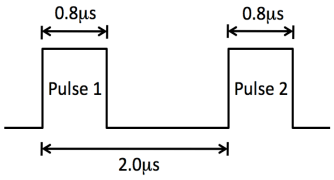

Figure 2: Signal Code Spacing Example

CALIBRATION VIA GPS

The primary purpose of radar calibration is to identify measurement biases and anomalous performance of radar stations[3]. Skin-tracking radar, which dates back to World War II[13], involves tracking and monitoring an object of interest by various radar stations distributed

throughout the world. The tracking data is then sent to a processing site, where the orbital data is computed[4].

A more recent evolution in orbital determination uses GPS receivers, particularly for satellites in LEO. Instead of relying on multiple Doppler stations to carry out the scheduling, tracking, and data transferring and processing, satellites with onboard GPS receivers can instead directly compute their own positions. The benefits of using a GPS receiver for orbital determination over ground Doppler stations include possible higher ephemeris accuracy and eliminating the reliance on numerous Doppler ground stations[3-4].

To accurately determine the location of an object using GPS, it is crucial that the GPS satellites know their own location, since all positional data is calculated with reference to the position of the GPS satellites. To do this, the GPS operational control segment collects tracking measurements on the GPS satellites using various tracking stations around the world. The data collected from those tracking measurements is then processed and estimates are then used to form "navigation messages", which are uplinked to the appropriate GPS satellites. Any GPS receivers within range of those GPS satellites will then receive these "navigation messages" that tells the users where the satellites are and they can then determine their own relative position[4].

CONCEPT OF OPERATIONS

Once Ho'oponopono is in orbit and within its required 10-degree pointing accuracy, the calibration process can take place. For the sake of simplicity, the entire process is described in two parts: experimental and ephemeris data collection.

The experimental data collection process begins with a calibration request from a radar station to the RADCAL coordinator at Vandenberg Air Force Base (VAFB). VAFB generates an interrogation schedule that is then sent to Ho'oponopono's ground station for uplinking. Creating interrogation schedules is crucial to ensure the transponder is not activated more than the five interrogations per day allotted by Ho'oponopono's power budget. The timing for the interrogation is derived using Two-Line Element (TLE) set calculations that help the station estimate when and where Ho'oponopono will pass. Once Ho'oponopono is within line-of-sight of the radar station, the interrogation process takes place.

The ephemeris data collection occurs simultaneously and begins with Ho'oponopono collecting GPS data using its zenith-facing GPS antenna. This GPS data is downlinked to Ho'oponopono's ground station, and made available to VAFB and the National Geospatial-Intelligence Agency (NGA). After processing the GPS orbital data, NGA makes the data available to a select group of users on the Internet, including the radar station requesting calibration.

After collecting both sets of experimental and ephemeris data, the radar station can correlate the two and quantify the accuracy of their system at identifying Ho'oponopono's position, and implement its calibration algorithms as needed.

HIGH-LEVEL REQUIREMENTS

At the root of Ho'oponopono's design are its system-level requirements. Its mission success criteria includes a set of requirements, most of which are customer-driven, that includes, but is not limited to:

- Collecting and disseminating ephemeris data with a minimum accuracy of 5 meters, which is the worst-case accuracy of the current RADCAL satellite[4].
- Activating the C-band transponder only prior to each requested use and deactivating it immediately thereafter. This is to ensure that power is not unnecessarily being consumed during non-interrogation periods[3].
- Operating the C-band transponder in both daylight and eclipse.
- Providing up to five transponder activations per day, every day for one year. The limitation is based on onboard power generation and storage.
- Ensuring a pointing accuracy of ± 10° within nadir. This is to ensure appropriate pointing of transponder and telemetry antennas for data uplinking and downlinking, beacon transmission, and transponder interrogations. This also ensures efficient GPS data collection for the zenith-facing GPS antenna.
- Collecting both L1 and L2 pseudorange and carrier phase measurements at a 30-second data rate, which is adequate for the required ephemeris collection.

As a participant in the AFOSR University Nanosatellite Program (UNP), Ho'oponopono's design is also constrained to program requirements that include[14]:

- Withstanding a static loading of 20 G's in both directions along all three principal axes of the satellite (*x, y, z*). Factors of safety (FOS) for the yield and ultimate loading cases shall not be lower than 2.0 and 2.6, respectively.
- Satellite structure must have a fundamental frequency of at least 100 Hz to ensure sufficient rigidity to survive a launch environment.
- Batteries must be contained in a battery box for thermal and structural protection.

- During ascent to orbit, air must be permitted to vent from the satellite in a manner that does not create excessive and potentially damaging depressurization forces.

Other constraints, e.g., fastener torque levels, must also be met as requirements set forth by NASA[15], which is providing Ho'oponopono's launch.

SYSTEM DESIGN

The elegance of Ho'oponopono's design is evident in comparing its ~3.5 kg mass to the original RADCAL satellite's 89 kg mass, all while having identical mission objectives. Additional advantages of Ho'oponopono's CubeSat implementation include significant reductions in development and launch cost.

Comprised of six essential subsystems, Ho'oponopono's design is conservative enough to fit a 3U CubeSat form-factor, yet comprehensive enough to incorporate important secondary features to ensure mission success. Its six subsystems are payload (PLD), attitude determination and control (ADCS), communications (COM), electrical power (EPS), command and data handling (CDH), and structure (STR).

Figure 3 is a block diagram of Ho'oponopono's subsystems showing their electrical connectivity through a common system bus.

Payload Subsystem

The PLD subsystem consists of a Herley MD2000C-1, a non-coherent transponder module that has a volume and mass of 13.8 cm^3 and 425 g, respectively. It operates using 22–32 VDC, and has an internal power supply that stabilizes transient voltages to the normal operating range. The transponder operates between 5.4–5.9 GHz, and is connected to a QHTF99R-5768 C-band quadrifilar helix antenna from the Antenna Development Corporation (Figure 4).

The PLD subsystem also includes a NovAtel OEMV-2-L1L2-F GPS unit and Antcom 1.9G1215A-XSO-2 antenna that are used for GPS data collection. The GPS unit, which runs on 3.3 VDC and has a mass of 56 g, is integrated on a printed circuit board (PCB) with a dsPIC33F microcontroller.

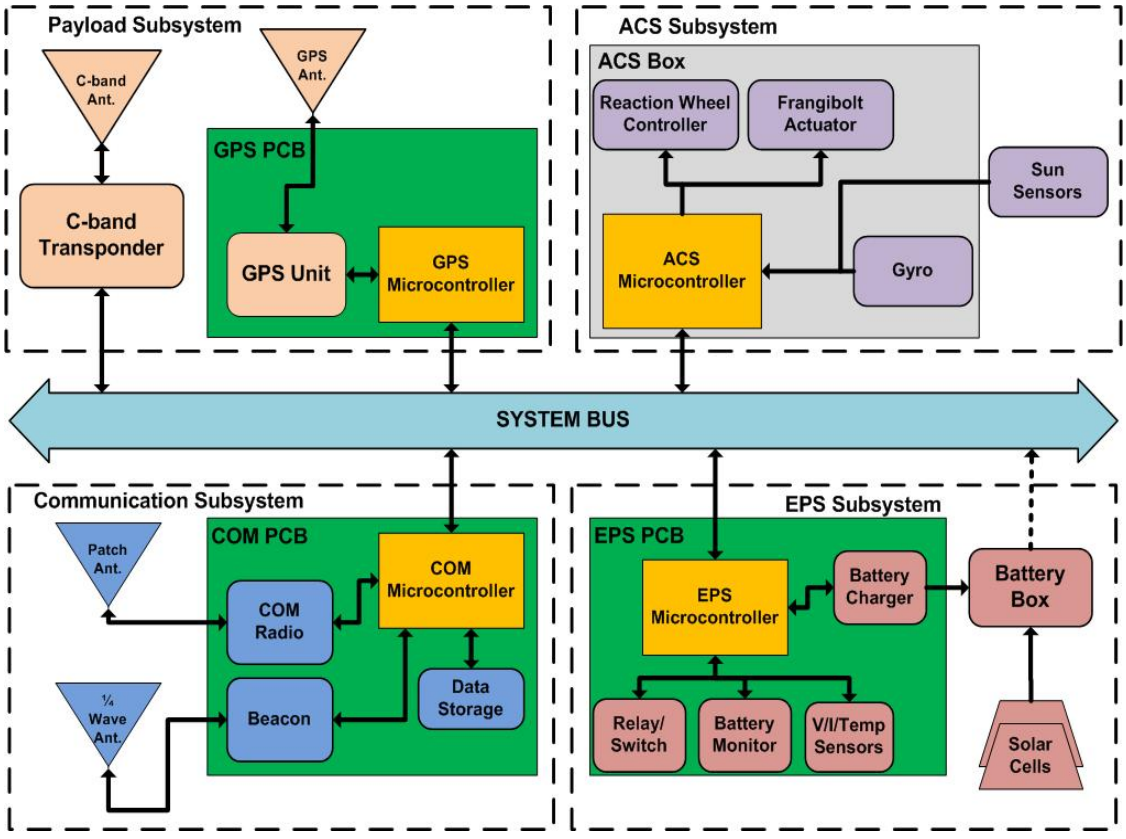

Figure 3: Block Diagram of Ho'oponopono System

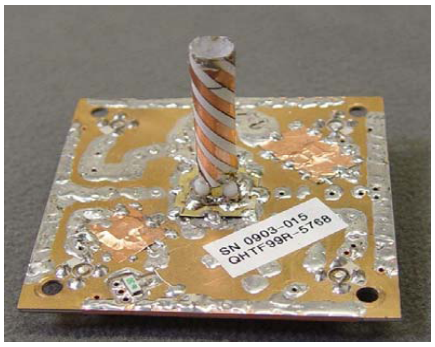

Figure 4: C-band Quadrifilar Helix Antenna

Attitude Determination & Control Subsystem

Ho'oponopono uses the Earth's gravity field to point its COM and PLD antennas in the nadir direction via a deployable gravity-gradient (GG) boom and attached endmass, shown in Figure 5. Unlike active-control schemes, gravity-gradient stabilization methods do not require a feedback control loop to adjust control torques to meet pointing objectives and therefore consume little power and do not require the design of a controller. A passive attitude control system design therefore tends to be simpler than an active one. However, a downside to GG stabilization is that a deployable is required, which introduces reliability concerns and requires extensive testing.

A 1-m deployable GG boom with an 80-g aluminum endmass (Figure 5) have been developed and successfully deployed in a 1-G environment. Modifications to this 1-m boom design are planned for the flight unit to allow the GG boom to have a 3-m extension, augmenting Ho'oponopono's pitch and roll inertia by over 200 times the retracted inertia about the pitch and roll axes to approximately 1.2 kg-m^2.

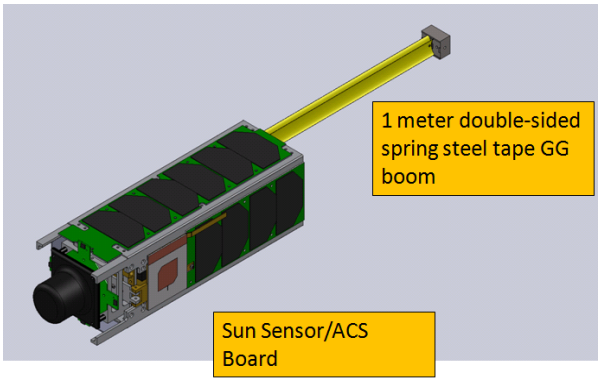

Figure 5: Ho'oponopono with GG boom Extended

Preliminary results indicate that this increase in inertia sufficiently reduces the nadir pointing error. Special consideration was taken to ensure the GG boom tether does not blossom due to vibration and to ensure little friction in the GG boom reel during extension. To overcome these issues, radial bearings are used as rollers that "cage" the tether in the radial direction yet provide a negligible tangential force that is nearly independent of the radial force. Although GG stabilization tests have not yet been performed due to their high difficulty, the design has been validated through simulation.

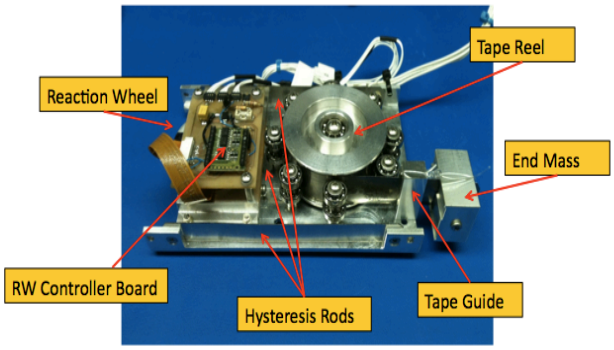

Figure 6: ADCS Subsystem

In the event that Ho'oponopono stabilizes in the wrong orientation, an EC 45 Flat motor reaction wheel from Maxon[16], shown in Figure 6, will rotate Ho'oponopono to the proper attitude. The motor is controlled by a Maxon DEC 24/2 speed controller that is integrated onto a custom PCB. A machined aluminum tape guide ensures that the boom extends along Ho'oponopono's long axis.

For attitude determination, Ho'oponopono uses an Invensense ITG3200 three-axis gyro[17] to measure rotation rates, a Honeywell HMC5843 magnetometer[18] to measure the magnetic field at the location of the satellite, and six OSI Optoelectronics S-100 photodiodes that act as sun sensors. Much of the development of the Kalman filter used to carry out these measurements is based on previous work done in this area[19-20].

Prior to deployment of the GG boom, Ho'oponopono must detumble to a low enough angular velocity to ensure that the GG boom will not buckle due to the deceleration as it is extended. Although an arbitrary number of conditions can be chosen to determine when the satellite has sufficiently detumbled, a velocity was chosen that corresponds to the satellite being captured in the GG field.

A MATLAB program was written to iteratively calculate the angular velocity norm. Figure 7 shows that an

angular velocity norm of approximately 0.645 deg/s is needed prior to extending the boom for GG capture in Ho'oponopono's tentatively planned 325-km orbit. Since the detumbling velocity for GG capture should be greater than the 0.066 deg/s orbit angular velocity, this indicates that the boom length is sufficient for the detumbling velocity requirement.

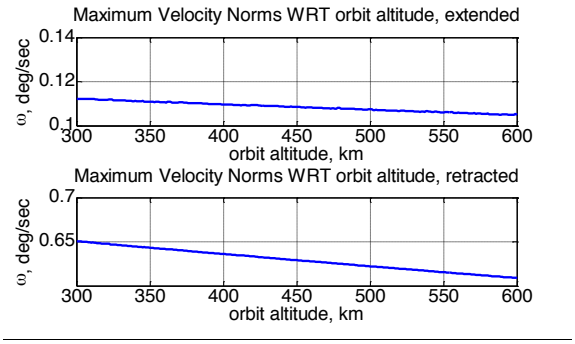

Figure 7: Required Angular Velocity Norm for Ho'oponopono at Various Orbits

Since the Earth's gravity field is conservative, it is not a reliable source for damping. Although atmospheric drag will certainly be present in Ho'oponopono's 325-km orbit, modeling this drag for simulation purposes is prone to error and therefore considered an unreliable source of damping. Although active detumbling schemes such as the B-dot control law are effective for high detumbling rates[21], these schemes consume power. Detumbling is therefore achieved using HyMu-80 hysteresis rods, shown in Figure 6, that also go by the trade name CO-NETIC, from the Magnetic Shield Corporation[22]. A single rod with a volume of approximately 0.96 cm^3 is placed parallel to each of the body axes of the satellite. Care is taken to ensure that the material retains its magnetic properties by not heating the material during machining. Hysteresis rods have significant flight heritage, as many of the early satellites launched in the 1960s were gravity gradient pointed and used hysteresis rods for oscillation dampening and kinetic energy dissipation.

The detumbling time is approximated through simulation by using a circular orbit model, along with hysteresis rod models provided from another simulation[23], at 325 km with a 40° inclination and initial tumbling velocity of 5 deg/s about each body axis. The time required for Ho'oponopono to detumble from the initial velocity to approximately 0.645 deg/s is estimated to be roughly three days, however further analyses are needed to validate this estimate.

After the hysteresis rods detumble the satellite, they are further required to dampen the oscillation of the satellite after the GG boom is extended. A thorough calculation has been performed and estimates an additional day is required for Ho'oponopono to stabilize within its required 10-degree pointing accuracy.

Communications Subsystem

Figure 8 shows the COM subsystem block diagram, with COM components in blue and supporting CDH components in orange. The COM subsystem includes a Microhard MHX2420-FT S-band radio with associated patch antenna and an AstroDev Neon-1 (Ne-1) UHF beacon with a quarter-wave monopole antenna. The COM subsystem is one of three subsystem PCBs in the PCB stack, the other two being the PLD and EPS subsystem PCBs. The PCB stack is connected through the system (SYS) bus, which is a 120-pin PC-104 connector.

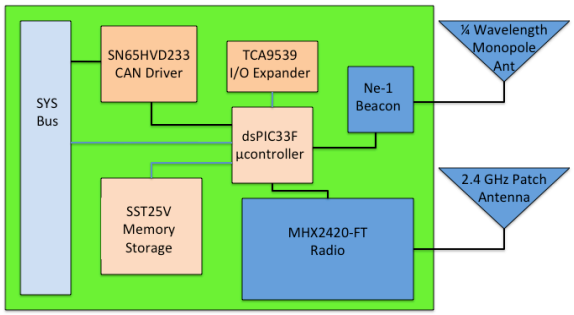

Figure 8: COM Subsystem Block Diagram

The radio and beacon are controlled by CDH's supporting hardware, which includes the Microchip dsPIC33F microcontroller[24], Texas Instruments (TI) TCA9539 I/O expander[25], TI SN65HVD233 CAN driver[26], and the Microchip SST25VF032B flash memory[27]. The dsPIC33F microcontroller controls the beaconing of SYS health data through the Ne-1 and the receive/transmit of data through the MHX2420. The MHX2420 receives uplinks of radar interrogation schedules as well as command and control data while transmitting collected GPS ephemeris data and satellite state of health.

COM, PLD, and SYS level requirements are the lead driving factors of the design. The COM subsystem requirements include having inhibits that prevent RF emission before deployment with a 45-minute delay, supporting sufficient uplink and downlink margins for all mission data elements, adhering to all spectrum licensing requirements, and ceasing all radio transmission at end of life.

The MHX2420-FT is a 2.4-GHz frequency-hopping spread-spectrum radio. The MHX2420 operates in the 2.4–2.4835 GHz range, and outputs 1 W of RF power with a required supplied voltage of 5 VDC[28]. COM operates the MHX2420 radio at a link rate of 57.6 Kbits per second to ensure adequate data bandwidth for the collected PLD GPS data, as described next.

Ho'oponopono's mission requirements include collecting both L1 and L2 pseudorange and carrier phase measurements every 30 seconds. The OEMV-2 outputs a Range Compressed data format, which contains the mission-critical GPS ephemeris data[29]. The nominal case of ten GPS satellites in view equates to a package size of 359 bytes collected every 30 seconds or 1,033 Kbytes of data per day. A minimum case of four GPS satellites in view gives a package size of 191 bytes, which is 550 Kbytes per day. Given the nominal case of 1,033 Kbytes per day, the COM radio link rate of 57.6 Kbits per second takes 2.4 minutes of downlink time per day. A link rate of 57.6 Kbits per second is an ideal data rate assuming Ho'oponopono's satellite passes average 5 to 10 minutes per pass.

The S-band microstrip patch antenna, shown in Figure 9, was designed to meet the required RF specifications[30]. The patch is fabricated on a Rogers 4350B substrate with a thickness of 60 mils and relative permittivity of 3.66[31]. A Digi-key J611-ND MCX RF connector was soldered at the feed point of the antenna.

Figure 10 shows the measured return loss (S11) of the patch antenna using a network analyzer and confirms the operating range to be 2.40–2.44 GHz. Additional return loss measurements at the C-band transponder frequencies confirm sufficient isolation at these frequencies, i.e., that the transponder doesn't unintentionally jam the S-band radio.

To measure the gain of the antenna, two identical patch antennas were fabricated and placed 1 m apart. One antenna was connected to a local oscillator transmitting at 13 dBm while the local oscillator frequency was varied over the range of 2.40–2.44 GHz. The received power was recorded and cable losses were taken into account. The Friis transmission formula was used to solve for the antenna gain. Maximum gain over the operable range of the antenna was found to be 5.31 dBi. Figures 11 and 12 show the measured radiation patterns.

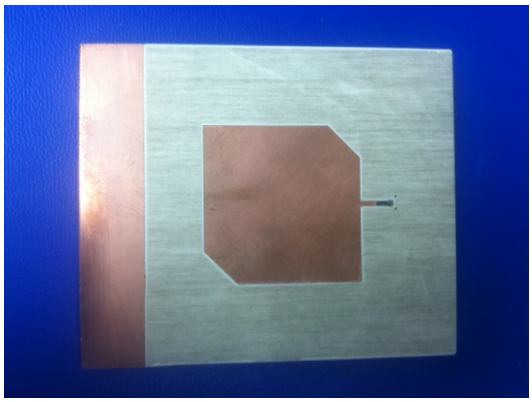

Figure 9: Fabricated S-Band Patch Antenna

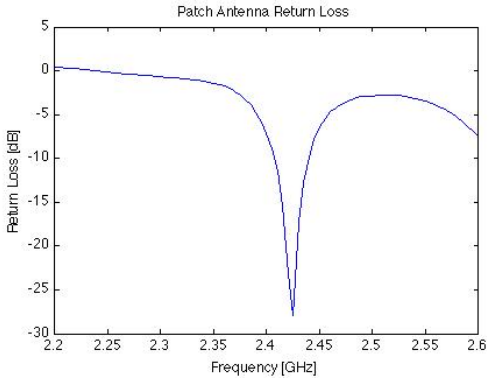

Figure 10: Return Loss vs. Frequency

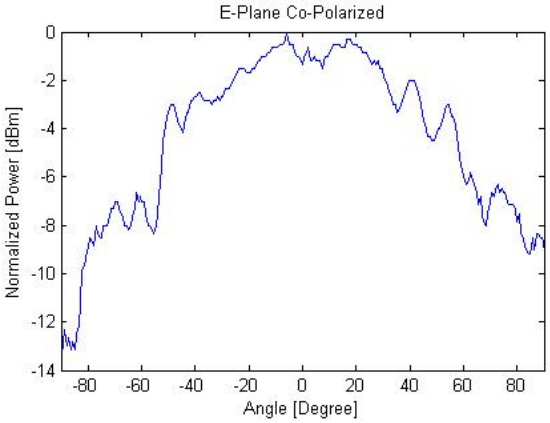

Figure 11: E-Plane, Co-Polarized

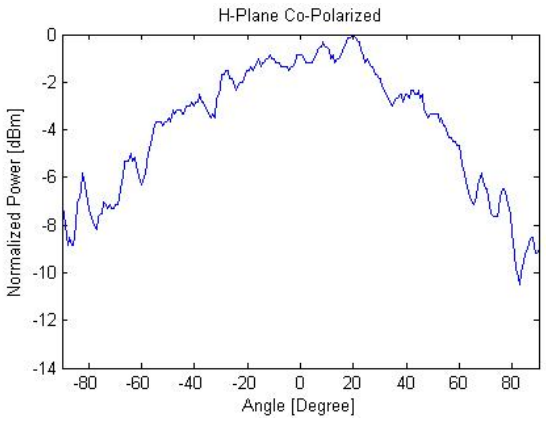

Figure 12: H-Plane, Co-Polarized

The AstroDev Neon-1 (Ne-1) is a miniature beacon used as a backup communication system capable of low data rates[32]. The Ne-1 beacon is capable of transmitting between 434–438 MHz; Ho'oponopono's exact beacon frequency is pending our assignment of a frequency license. The beacon has an RF output of 0.8 W with a DC power consumption of approximately 2.4 W. The beacon communicates using AX.25 packet protocols or also configurable CW modes. Once Ho'oponopono is inserted into orbit and the batteries are charged, CDH commands on the beacon to inform ground users of its health status. The Ne-1 is capable of sending a packet size of 250 bytes, which will be used to send state-of-health data such as temperatures, voltages, currents, and operation modes of critical components.

The beacon link budget was conducted at multiple elevation angles for a 325-km orbit altitude. The link budget calculations assume an Ne-1 beacon RF output power of 0.8 W transmitting to UH's UHF ground station[33]. The downlink margins for the best- and worst-case scenarios are summarized in Table 1. The best-case downlink margin assumes a 2-dB beacon antenna gain, 1-dB line loss, 3-dB polarization and propagation loss, and 1-dB implementation loss.

Other uplink data that may be required is the reprogramming of a dsPIC33F microcontroller. The dsPIC-33F microcontroller has a program flash of 128 Kbytes[34]. This would take on the order of 2.2 seconds to uplink with a data rate of 57.6 Kbits per second.

Table 1: Beacon Link Budget Summary

325 km Orbit	Downlink Margin (best-case)
10° elevation angle	8.5 dB
20° elevation angle	13.6 dB
30° elevation angle	17.8 dB
90° elevation angle	29.4 dB

Electrical Power Subsystem

The EPS is designed to meet the power requirement needs of the various commercial-off-the-shelf (COTS) components distributed throughout Ho'oponopono's system bus. The ability to activate the Herley MD2000C-1 transponder five times per day, along with the transponder's 7-W power requirement, were driving factors to implement a large power margin as well. A block diagram of Ho'oponopono's EPS is shown in Figure 13.

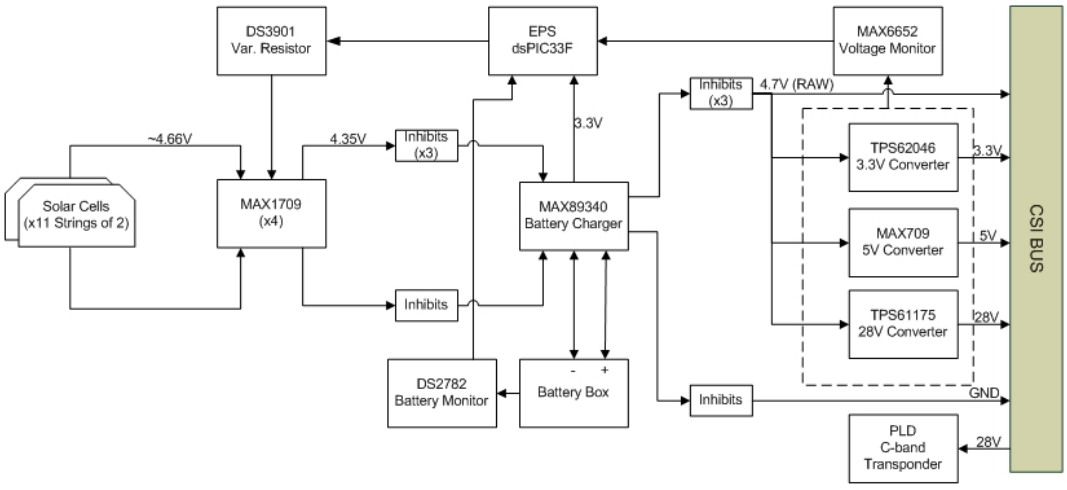

Figure 13: EPS Block Diagram

Power is generated through use of Emcore 609147-BE Triple-Junction Monolithic Diode (BTJM) solar cells with 28% efficiency. This relatively new photovoltaic technology offers improved radiation hardness while reducing the required surface area coverage and increasing the potential mission lifetime as well. Six solar cells are distributed along three of Ho'oponopono's four lateral faces. A 2.4-GHz deployable patch antenna mounted to the remaining lateral face limits the surface area to fit four cells, for a total cell count of 22. The cells along each solar panel are arranged in pairs that are wired in series. These pairs are then all connected in parallel, as shown in Figure 14.

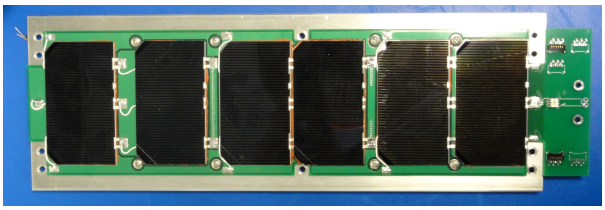

Figure 14: Solar Cell Configuration

The output from each solar panel is fed to a Maxim MAX1709 DC/DC converter with 90% efficiency, which is integrated on the inside of each panel. The output from the MAX1709 converter is controlled using its feedback pin and a Maxim DS3901 variable resistor, whose voltage divider resistance values are chosen to provide a constant 4.35 VDC. This output voltage powers a MAX8934D Li+/Li-Poly linear battery charger.

The battery charger, which features temperature-monitoring capabilities during periods of charging and discharging, provides a range of voltages (3–4.35 VDC) and has three output options. The 'Always-On Linear Regulator Output' pin provides a constant 3.3 VDC with 30 mA, which powers the EPS dsPIC33F microcontroller. The 'System Supply Output' is the other pin that is used to output either a regulated (3–4.2 VDC) Li-Poly battery voltage or a regulated 4.35 VDC.

The RAW output voltage from the MAX8934D battery charger is fed to three converters to provide 3.3 VDC, 5 VDC, and 28 VDC, and also supplied to the system bus for distribution to COM, PLD, and ADCS. The Texas Instruments TPS62046 DC/DC converter outputs 3.3 VDC and has a maximum output current of 1.2 A. The MAX1709 DC/DC converter boosts the RAW voltage up to 5 VDC with a maximum output current of 5 A. Two TPS61175 DC/DC converters are cascaded in series to provide the 28 VDC and 7 W required for the Herley MD2000C-1 transponder module.

The EPS Microchip dsPIC33F microcontroller, when used in normal operations, is able to implement peak power tracking through control of the DS3901 variable resistor. Further research is needed to determine the necessity for peak power tracking. In the event that the EPS batteries discharge to non-operational levels, the dsPIC33F maintains control by operating the satellite system in a "power save" mode until the batteries charge to a nominal level.

Power is stored using 15 COTS Tenergy Li-Polymer 3.7-V 1150-mAh batteries. These batteries are spot welded together in parallel and provide 3–4.2 VDC, depending on their level of discharge, with a storage capability of 62 Wh.

Ho'oponopono's battery box is a machined aluminum enclosure with six exterior venting holes covered with a fine-weaved mesh material for venting and electrolyte leakage prevention. An 0.08-inch-thick Nomex[35] absorbent material is used to fill all internal voids as well as contain any electrolyte leakage, while a fuse and thermistor are implemented for safety and ground servicing. This design follows all UNP-6 requirements.

Two identical inhibit schemes, also shown in Figure 13, have also been implemented as a UNP-6 requirement to prevent prelaunch electrical activity. Each inhibit scheme consists of four Panasonic TX2SL-LT-4.5V-TH relays. The first set of relays is deactivated once Ho'oponopono separates from its Poly Picosatellite Orbital Deployer (P-POD) and a Cherry E62-60K separation switch is no longer depressed. The second set is deactivated by the EPS microcontroller once the battery is charged to a required level.

To ensure that Ho'oponopono will operate properly throughout mission operations, the EPS features power-monitoring capabilities that not only detect flags and alerts of the MAX8934D battery charger and various voltage converters, but also monitors the Li-Polymer battery and bus voltage lines. The DS2782 battery monitor measures a fuel gauge of the batteries charge levels to ensure proper cell management. A MAX6652 voltage monitor is also implemented to measure the 3.3, 5, and 28 VDC lines.

Command and Data Handling Subsystem

The basis of Ho'oponopono's CDH architecture is UH's CubeSat Stackable Interface (CSI)[36-37], which was developed to provide a cleaner EPS subsystem. CSI minimizes the need for a complex wiring scheme to distribute voltages across a PCB stack by providing standardized voltages across a common bus. CSI uses the PCI-104 standard that not only provides a robust connection, but also fits within a 1U CubeSat form fac-

tor. A key feature of CSI is the option to place addressable I/O expanders on each board in the stack to be accessed by an I2C bus, which allows for remote access for a multitude of I/O in the system. The further addition of on/off switches controlled by this I/O expander allows for a remote power management system that is controlled by two lines across CSI as shown in Figure 15.

CSI also supports four levels of data communication as shown in Figure 16. At the lowest level, 32 digital I/O pins allow for point-to-point communications between devices on the bus. Four UART channels form a secondary level of point-to-point communication. The main communication bus uses Controller Area Network (CAN) for robust data transfer. CAN uses an arbitration system that minimizes collisions on the network and also allows for low-power data transfer by taking advantage of differential signaling. CSI also supports USB channels that are not used in Ho'oponopono.

The CAN bus allows multiple nodes to communicate using a wait-on-send approach. There are predetermined time slots in which a transfer can occur, and at the beginning of these time slots is an arbitration period in which each device on the bus wanting to transmit sends its message identifier. In arbitration, if two or more devices wish to start a transfer at the same time slot, each device will start transmitting its arbitration sequence and the higher priority message will be sent. Each message type has its own unique label in arbitration ensuring that no collisions will occur[38].

CDH relies on supporting component hardware to maintain control of each subsystem. CDH's component integrated circuits (ICs) include: the Microchip dsPIC33F microcontroller, Texas Instruments (TI) TCA9539 I/O expander, TI SN65HVD233 CAN driver, and the Microchip SST25VF032B flash memory. The microcontroller selected from the Microchip dsPIC33F family is the dsPICFJ128MC804 which has an on-chip flash program memory of 128 Kbytes, supports one I2C, two UART, and two SPI digital communication peripherals[39]. This microcontroller also supports an enhanced CAN module that has up to eight transmit and up to 32 receive buffers[40]. TI TCA9539 I/O expanders each have a low standby-current consumption of 3 µA while also each featuring 18 5-V tolerant I/O ports[41]. Using the I2C protocol, these I/O expanders give the EPS microcontroller remote access to all of its I/Os across the CSI bus. Selected to operate in especially harsh environments, the TI SN65HVD233 CAN drivers provide transmit and receive capabilities between the differential CAN bus and CAN controllers, with signaling rates up to 1 Mbps[42]. Ho'oponopono's CAN drivers manage the robust CAN bus ensuring a clean bus for data transfer between the subsystem microcontrollers. CDH has two Microchip SST25VF032B flash memories, featuring a four-wire, SPI-compatible interface, having each 32 Mbits of flash memory[43].

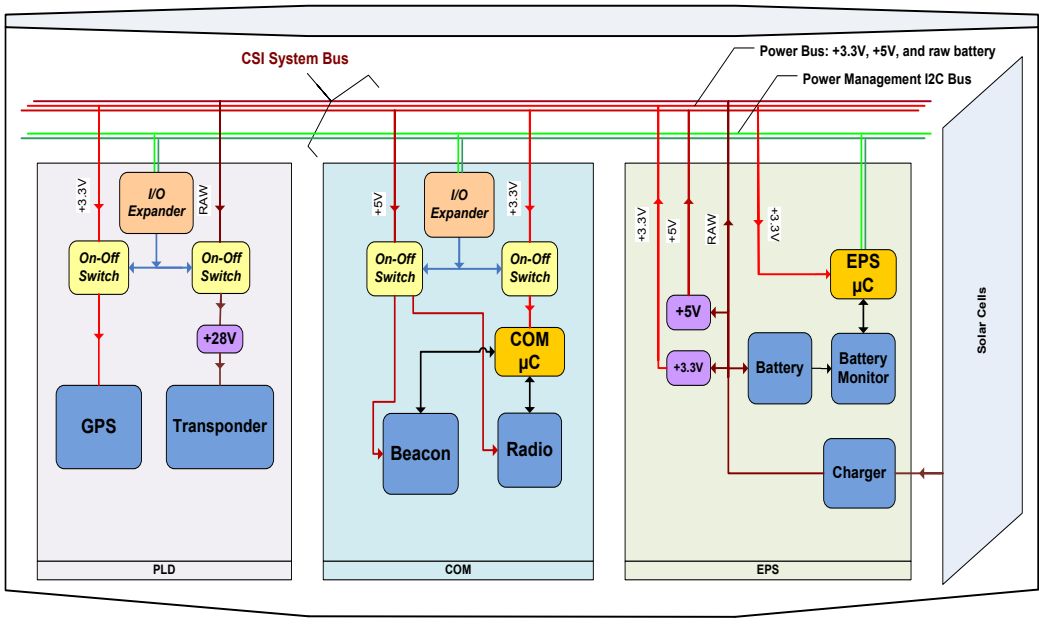

Figure 15: Block Diagram of CSI Architecture

	A		B		C		D		
1	USB_N	GPS (PLD)	GND	GND	GND	GND	USB_P	GPS (PLD)	1
2	GND	GND	GND	GND	GND	GND	GND	GND	2
3	PM_SCL	PICs & I/O Exps	PM_SCL	PICs & I/O Exps	PM_SDA	PICs & I/O Exps	PM_SDA	PICs & I/O Exps	3
4	CAN_HI	CAN Drivers	CAN_HI	CAN Drivers	CAN_LO	CAN Drivers	CAN_LO	CAN Drivers	4
5	+3.3V	+3.3V	+3.3V	+3.3V	+3.3V	+3.3V	+3.3V	+3.3V	5
6	+3.3V	+3.3V	+3.3V	+3.3V	+3.3V	+3.3V	+3.3V	+3.3V	6
7	GND	GND	GND	GND	GND	GND	GND	GND	7
8	RAW	+4.7V	RAW	+4.7V	RAW	+4.7V	RAW	+4.7V	8
9	RAW	+4.7V	RAW	+4.7V	RAW	+4.7V	RAW	+4.7V	9
10	RAW	+4.7V	RAW	+4.7V	RAW	+4.7V	RAW	+4.7V	10
11	GND	GND	GND	GND	GND	GND	GND	GND	11
12	TXD_A	Radio (COM)	TXD_B	Beacon (EPS)	TXD_C	GPS (PLD)	MISO	Flash Mem (COM)	12
13	RTS_A	Radio (COM)	RTS_B		RTS_C	GPS (PLD)	MOSI	Flash Mem (COM)	13
14	RXD_A	Radio (COM)	RXD_B	Beacon (EPS)	RXD_C	GPS (PLD)	SCK	Flash Mem (COM)	14
15	CTS_A	Radio (COM)	CTS_B		CTS_C	GPS (PLD)	!CE1	Flash Mem (COM)	15
16	GND	GND	GND	GND	GND	GND	GND	GND	16
17	RA0	Radio DCD (COM)	RB0	COM !MCLR	RC0	EPS !MCLR	RD0	!CE2 (COM)	17
18	RA1	IOX Alert (COM)	RB1	COM PDG	RC1	EPS PDG	RD1	12V_TM (PLD)	18
19	RA2	IOX Alert (EPS)	RB2	COM PGC	RC2	EPS PGC	RD2		19
20	RA3	IOX Alert (PLD)	RB3	GPS !MCLR	RC3		RD3		20
21	RA4	ACS IO (reserved)	RB4	GPS PDG	RC4		RD4		21
22	RA5	ACS IO (reserved)	RB5	GPS PGC	RC5		RD5		22
23	RA6	ACS IO (reserved)	RB6		RC6		RD6		23
24	RA7	GPS PPS (PLD)	RB7		RC7		RD7		24
25	GND	GND	GND	GND	GND	GND	GND	GND	25
26	+5V	Beacon & Radio	+5V	Beacon & Radio	+5V	Beacon & Radio	+5V	Beacon & Radio	26
27	+5V	Beacon & Radio	+5V	Beacon & Radio	+5V	Beacon & Radio	+5V	Beacon & Radio	27
28	GND	GND	GND	GND	GND	GND	GND	GND	28
29	SC_IN	+4.35V	SC_IN	+4.35V	SC_IN	+4.35V	SC_IN	+4.35V	29
30	SC_IN	+4.35V	SC_IN	+4.35V	SC_IN	+4.35V	SC_IN	+4.35V	30

Figure 16: CSI Pin Layout

An important aspect of CDH is the ability to ensure sufficient data storage as this is the driving factor in Ho'oponopono's mission. The primary payload data is the GPS ephemeris that will be stored on Microchip SST25V032B memory chips. These flash memory chips, in conjunction with the Microchip dsPIC33F's internal memory, allow 64 Mbits of data[44] to be stored which, in the extreme case of each GPS packet being 847 bytes, allows 9904 packets to be stored. At a GPS ephemeris collection rate of 30 seconds per packet, Ho'oponopono can store up to 3.4 days worth of data.

Ho'oponopono's CDH software is based on a four-level programming model for the subsystem microcontrollers distributed across the CSI bus.

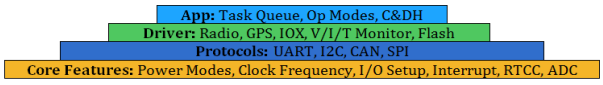

Figure 17: Four-Level Programming Model

The first level, starting at the base of Figure 17, is the core features layer. The core features for the dsPIC33F microcontroller include power modes, clock frequency, setup of I/O ports, interrupts, real time clock and calendar (RTCC), and analog to digital conversion (ADC). Next, moving up one level to the protocols layer, the UART, I2C, CAN, and SPI protocols are developed in software to be callable functions. These functions are called upon by the driver layer that is developed for the COM radio, PLD GPS, TCA9539 I/O expanders, voltage, current, and temperature monitors, and the SST25VF032B flash memory. The driver layer tells the protocols how to function based on parameters such as data rate and I/O setup. The final programming layer is the application layer, and includes task queue, operation modes, and command and data handling. The application layer is developed uniquely for each of the subsystem microcontrollers.

Structure Subsystem

From a general standpoint, the structural subsystem of Ho'oponopono must fulfill the basic requirements of a satellite structure, namely surviving launch loads and the on-orbit environment. Being a 3U CubeSat, the structural subsystem must match the CubeSat form factor, allowing it to be deployed from the PPOD. Accordingly, the overall structural envelope and mass properties were made to conform to the Cal Poly standard[45]. Beyond these requirements, the satellite structure is responsible for providing appropriate mounting points both internally and externally for the other subsystems.

Ho'oponopono's structure was designed with subsystem and UNP requirements in mind. Beyond strength requirements, mission and program requirements were followed which dictated the placement of various subsystems and components such as the payload and communications antennas. To this end, the C-band transponder antenna needed to be mounted to one end of the 3U CubeSat with the GPS antenna on the opposing end. Additionally, the need for an S-band patch antenna as well as a radio beacon antenna meant that a deployable mechanism was required.

The first option explored was to use a COTS CubeSat Kit structure from Pumpkin[46]. However, the mounting locations of the COTS structure were not sufficient for our payload or PCB stack, and so extensive modification and/or adapting of the structure with custom mounting brackets would have been required.

It was therefore deemed necessary to create a custom CubeSat structure to fit the mission needs. For this purpose, the structure from a previous UH CubeSat, Ho'okele, was used as inspiration[47]. The basic chassis design consists of four walls: two are flat and two are bracket-shaped, having right angle tabs where the flat walls attach to hold the two sides together. End brackets enclose the CubeSat structure.

The structural design was performed primarily via SolidWorks CAD. Existing models of payload components and other subsystems were used to design the encompassing satellite structure. The process was highly iterative, with unforeseen requirements and conflicts continually arising that required design modification or,

in some cases, complete redesign of certain parts. Placement of subsystem mounting locations required input and feedback from the various subsystem teams and systems engineers. Along with the aforementioned antenna placement requirements, subsystem input was needed to determine the PCB stack order and placement, along with payload location and orientation.

Another consideration in this area was cabling, as the four antennas on Ho'oponopono required extensive RF and power cable routing along the interior of the satellite. The exterior of the structure also needed to mount solar panels.

Finally, the deployables were sited in accordance with COM and ACS subsystem requirements for deploying the patch antenna and gravity gradient boom, respectively.

Ho'ponopono's chassis took all of these requirements into consideration and was designed to be an aluminum skeleton that provided strength and support while also minimizing overall mass and balance. Figure 18 shows a CAD model of the finished structural assembly. The similarities of our basic chassis design to the CubeSat Kit can be noted, as well as the need for an entirely custom satellite structure to meet our mission and program requirements.

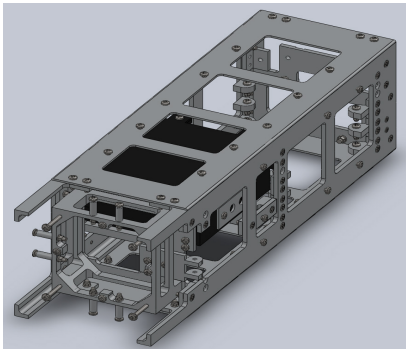

Figure 18: SolidWorks Model of Ho'oponopono Structure

Load paths were qualitatively considered in creating the shape and form of the chassis components; this meant placing ribs and struts symmetrically whenever possible. Generous fillets were used to avoid high stress concentrations, usually 1/8 inch. To this end, all mounting holes were placed at least 1.5 diameters from the edges of components in order to further ensure low stress concentrations. The bracket walls, to which most of the internal components were mounted, were made to be thicker than the flat walls that braced them to ensure strength, rigidity, and low stress concentrations around joints.

Several standards and rules of thumb guided the development of the design. First, only mil-spec fasteners were used. Due to the size and intricacy of our structural design, mostly #4-40 screws were utilized. Mil-spec deformed thread lock nuts were also chosen to ensure fastener retention. Second, nutted joints were utilized for all critical structural joints, namely those joining chassis components. For non-critical joints, tapped holes and Helicoil inserts were used. A minimum of five threads of engagement was required for each non-critical joint, meaning that components less than 1/8 inch thick would not be tapped.

After finalizing a structural design meeting all internal requirements, SolidWorks FEA simulations were used for dynamic and stress analyses to ensure the design met UNP strength requirements. Simulations of each of the six loading scenarios dictated by the UNP (20 G's: *+/- x, +/- y, +/- z*) were performed. Table 2 summarizes the results of these simulations, and shows minimum yield and ultimate FOS values of 4.90 and 5.52, respectively. These values exceed the 2.0 yield and 2.6 ultimate FOS values prescribed by the UNP.

Table 2: Predicted Yield and Ultimate FOS Values for Six Loading Scenarios

Inertial Loads (G's)			Factor of Safety (FOS)	
x	*y*	*z*	Yield	Ultimate
20.0			4.90	5.52
-20.0			5.04	5.67
	20.0		15.49	17.42
	-20.0		13.72	15.44
		20.0	13.32	14.99
		-20.0	13.58	15.28

Figure 19 shows the results of the *x*-direction load case simulated with all stress levels indicated by the color code. A SolidWorks frequency simulation found the fundamental frequency of Ho'oponopono's structure to be 1.6 kHz.

To meet the UNP depressurization requirement, six venting holes were placed in the sides of the battery box. A venting analysis was performed to ensure that the battery box depressurized with a FOS of at least 2.0, per the UNP requirement. This analysis was guided by an AIAA publication regarding Space Shuttle payload venting[48]. An FOS of 24 was calculated for the lid of the battery box and an FOS of 105 was calculated for the box itself. Figure 20 shows the result of an accompanying FEA simulation.

All structural components were milled out of 6061-T6 aluminum except the deployable patch antenna cradle hinge, which was machined out of brass for solderability. For the larger and more intricate parts, such as chassis walls and brackets, a CNC mill was used. Some smaller parts were machined by hand for the engineering design unit, with the intention of machining all flight parts on a CNC machine.

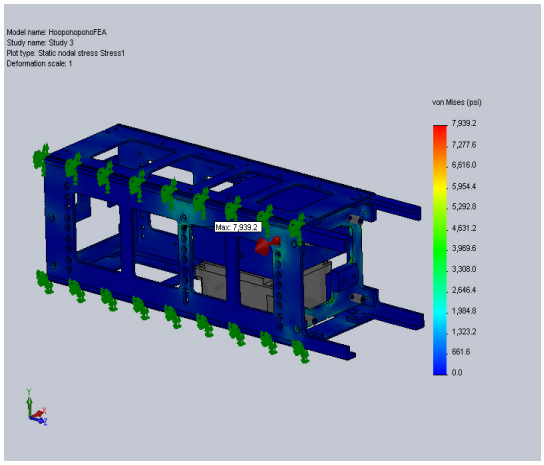

Figure 19: Static Load FEA Simulation Showing Stress Levels on Ho‘oponopono’s Structure

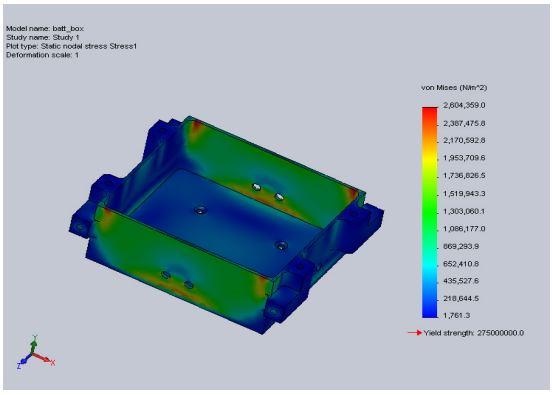

Figure 20: SolidWorks FEA Simulation Showing Depressurization-Induced Stresses

Fasteners, having been specified from the CAD assembly for type, size, and length, were ordered from Arizona Industrial Hardware. Assembly of the satellite chassis as well as subsystem and payload mounting were performed according to an internal assembly procedure document[49]. Specific torque levels for fasteners were imparted using a Snap-On QDRIVER3 torque screwdriver. Fit checks revealed that all subsystem components fit within tolerances. Additionally, a fit check of the satellite bus within a P-POD prototype demonstrated similar compliance.

TESTING

Ho‘oponopono will undergo vibration testing to simulate expected launch loads. A maximum acceleration of 20 G’s is assumed, in accordance with UNP requirements. NASA requirements also dictate that Ho‘oponopono have no observable yield failure at a loading of 22 G’s and no observable ultimate failure at 25 G’s[50].

Although higher fidelity thermal tests are planned, a preliminary, spherical model analysis was carried out with presumed steady-state temperature fluctuations of -66 °C in eclipse to 76 °C in the sun[17]. In-flight temperature measurements from previous Cal Poly CubeSats, however, suggest that the actual temperature range will be closer to 0 °C in eclipse and 70 °C in the sun. A higher fidelity Thermal Desktop model is being developed to determine whether these temperature ranges are accurate.

Qualification testing of structural parts has yet to be performed but test plans have been conceived of and are being finalized with the guidance of NASA environmental testing standards[51].

Tests are planned to measure the radiation pattern of the S-band patch antenna when fully integrated onto the satellite structure. Thorough testing of the monopole antenna will also ensure proper operations of the Ne-1 beacon when Ho‘oponopono is detumbling or stabilized in orbit.

A series of tests are planned to validate the performance and functionality of the voltage converters, battery charger, and batteries of Ho‘oponopono’s EPS. A load board, shown in Figure 21, made with an array of LEDs was designed to act as a variable load that will mock different load scenarios, e.g., transponder interrogations.

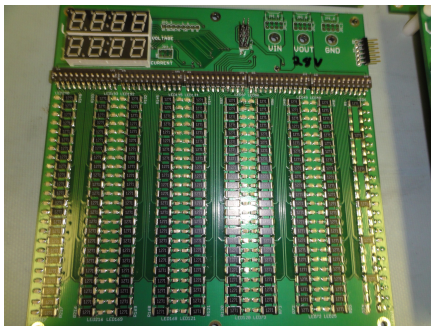

Figure 21: EPS Testing Load Board

Electromagnetic interference tests will also be conducted to characterize the effects of Ho‘oponopono’s RF and electrical sources.

UNP INVOLVEMENT AND FUTURE LAUNCH

Ho'oponopono and its mission were the basis for UH's participation in the 2009-2011 UNP-6, an Air Force-funded satellite design and fabrication competition. In completing this rigorous, two-year competition, Ho'oponopono's design went through a six-level review process (Proposal Merit Review, Systems Concept Review, Systems Requirements Review, Preliminary Design Review, Critical Design Review, Proto-qualification Review) that was judged by DoD, NASA, and industrial reviewers. Throughout these reviews, Ho'oponopono's design was judged on its technical merit, educational merit, and feasibility. Independent design evaluations were also held with review boards consisting of engineers from Northrop Grumman Aerospace Systems and InDyne Inc.

After the final UNP Flight Competition Review in January 2011, the team brought home the Most Improved and Third Place Awards[52-53].

Knowing beforehand that the UNP would only select one nanosatellite for launch by the Space Test Program, UH chose to fulfill its mission within a CubeSat form factor so that it could pursue other launch opportunities if it didn't win first place. In fact, this was our philosophy behind choosing a CubeSat mission for UNP-3 as well. This strategy paid off when in February 2011, NASA announced that Ho'oponopono was one of 20 CubeSats selected to fly as auxiliary cargo onboard rockets planned to launch in 2011 and 2012 as part of the Educational Launch of Nanosatellites Program[54], and is tentatively manifested for an August 2012 launch as part of the Commercial Resupply Services 3 payload aboard a SpaceX Falcon 9 rocket. The tentative launch parameters include a 350 km elliptical orbit with 51° ± 2° inclination[55].

EDUCATIONAL VALUE

One of the most notable aspects of the Ho'oponopono project is that while it is faculty-guided, it is predominantly student-driven[56]. In fact, undergraduate students have led the development efforts for all seven of UH's eight CubeSat projects to date[57].

This is directly in line with the goals of the UNP: ensuring students are the ones leading all facets of the project, from program management, to the design, fabrication, and testing of a full-fledged satellite. Students are also required to follow meticulous documentation guidelines, as well as create and submit deliverables that they must present to professional reviewers. Students have also made several presentations to Air Force officials both at the UH campus and VAFB. This all provides for valuable experiences that few engineering students can appreciate – a taste of the common practices in government and industry projects and a jump start on practical engineering experience.

CONCLUSIONS

This paper presented the first radar calibration satellite in a CubeSat form factor, demonstrating the ability of a university student team to address an urgent operational need at very low cost while simultaneously providing immense educational value. Design considerations for all of the major subsystems were discussed, in the context of meeting the requirements for this mission. Our team is approximately one year away from launch, and we are certain that we'll be learning as much in that upcoming one year as we have in the past two years designing the satellite.

ACKNOWLEDGEMENTS

The authors express their deepest gratitude to the following organizations and individuals:

- Air Force University Nanosat Program (particularly Abbie Stovall, Jared Clements, David Voss, Kelly Cole, Kent Miller, and all of the external reviewers) for providing the amazing opportunity to design, construct, and test our satellite;
- NASA Educational Launch of Nanosatellites Program (particularly Garrett Skrobot) for providing the even more amazing opportunity to launch it;
- Martin Prochazka and his entire team at InDyne/WROC for mentoring on the mission-related aspects of our project, as well as Vandenberg Air Force Base 30th Space Wing and Naval Postgraduate School for providing government-furnished equipment and materials;
- Nolan Tanaka and his whole team at Northrop Grumman, Roland Coelho and Jordi Puig-Suari of Cal Poly San Luis Obispo, Gerry Shaw of SRI, and James Cutler of University of Michigan, for invaluable advice and support;
- Northrop Grumman, Boeing, and the UH College of Engineering for providing financial support;
- Byron Wolfe, Jason Akagi, Lance Yoneshige, Monte Watanabe, Justin Akagi, Alex Zamora, Tyler Chun – all past students of our UH Small-Satellite Program - for mentoring the current students in our program;
- Jason Axelson, Shantel Hunt, Toy Lim, Joseph Longhi, and the dozens of other students past and present who directly contributed to Ho'oponopono;

We could not have gotten this far without each one of you.

REFERENCES

1. Kramer, H. J., Observation of the Earth and its Environment – Survey of Missions and Sensors, 2nd ed., Springer-Verlag, pp. 1492-1493, May 1994.
2. "Defense Meteorological Satellite Program (DMSP) Satellite F15," National Snow and Ice Data Center, http://nsidc.org/data/docs/daac/f15_platform.gd.html
3. Langer, J. V., Feess, W. A., Hanington, K. M., Bacigalupi, M. R., Cardoza, M. A., Mach, R. G., and Abusali, P. A. M., "RADCAL: Precision Orbit Determination with a Commercial Grade GPS Receiver," Proceedings of the 1994 National Technical Meeting of The Institute of Navigation, San Diego, CA, January 1994, pp. 421-431.
4. Langer, J., Powell, T., and Cox, J., "Orbit Determination and Satellite Navigation," Aerospace Corporation Website, May 11, 2007. http://www.aero.org/publications/crosslink/summer2002/04.html
5. Prochazka, M., RADCAL Coordinator at Vandenberg Air Force Base, personal communication.
6. "Joint Space Operations Center," Vandenberg Air Force Base Website, June 06, 2008, http://www.vandenberg.af.mil/library/factsheets/factsheet.asp? id=12579
7. "JSpOC Increases Tracking Capabilities," Air Force Space Command Website, September 01, 2009, http://www.afspc.af.mil/news/story.asp?id=123165722
8. Dorf, R. C., The Engineering Handbook, 2nd Edition, CRC Press, pp. 138-5 – 138-6, 2005.
9. Wolff, C., "Concept of Coherence," http://www.radartutorial.eu/11.coherent/co05.en.html
10. Wehner, D. R. 1931. High-Resolution Radar, 2nd ed., Artech House, pp. 15, May 2011.
11. "Defeating Theatre Missile Defense Radars with Active Decoys," Science and Global Security, vol. 6, pp. 333-355, 1997. http://www.princeton.edu/sgs/publications/sgs/pdf/6_3frankel.pdf
12. Rogers, T., "Transponder Basics," AVWeb http://www.public-action.com/911/transpon/
13. "The History of Radar," British Broadcasting Corporation Website, July 14, 2003. http://www.bbc.co.uk/dna/h2g2/A591545
14. University Nanosatellite Program 6 User's Guide
15. "Standard, Threaded Fasteners, Torque Limits For," Document ID MSFC-STD-486B, https://standards.nasa.gov/documents/detail/3314929
16. Maxon Motors Website, http://www.maxon-motor.com/
17. Wertz, J. R. and Larson, W. J., Space Mission Analysis and Design, Microcosm Press, 1999.
18. http://www51.honeywell.com/aero/common/documents/myaerospacecatalog-documents/Defense_Brochures-documents/HMC5843.
19. Svartveit, K., Attitude Determination of the NCUBE Satellite, Norwegian University of Science and Technology, Masters Thesis, 2003. http://www.itk.ntnu.no/ansatte/Gravdahl_Jan.Tommy/Diplomer/Svartveit.pdf
20. Psiaki, M., "Three Axis Attitude Control Determination via Kalman Filtering of Magnetometer Data," Journal of Guidance, Control and Dynamics, vol. 13, May-June 1990.
21. Flatley, T.W., Morgenstern, W., Reth, A., and Bauer, F., "A B-Dot Acquisition Controller for the RADARSAT Spacecraft," Guidance, Navigation and Control Branch, Goddard Space Flight Center.
22. Magnetic Shield Corporation Website, http://www.magnetic-shield.com/
23. Park, G., Seagraves, S. and McClamroch, N.H., "A Dynamics Model of a Passive Magnetic Attitude Control System for the RAX Nanosatellite," AIAA Guidance, Navigation, and Control Conference, 2010.
24. http://www.microchip.com/wwwproducts/Devices.aspx?dDocName=en532303
25. http://focus.ti.com/docs/prod/folders/print/tca9539.html
26. http://focus.ti.com/docs/prod/folders/print/sn65hvd233.html
27. http://www.microchip.com/wwwproducts/Devices.aspx?dDocName=en549421
28. MHX2420 datasheet, MHX2420.Brochure.Rev.3.11.pdf
29. OEMV Firmware Reference.pdf, pg. 403-405.
30. Balanis, C. A., Antenna Theory: Analysis and Design, 2nd ed., John Wiley & Sons, 1996.
31. http://www.rogerscorp.com/acm/index.aspx
32. http://www.astrodev.com/public_html2/downloads/datasheet/Ne1UserManual.pdf

33. Ichikawa, D. J., Iwami, R. T., Rodrick, R. J., Akagi, J. M., and Shiroma, W. A., "Ground Station Design: The Mobile Approach," in The Emergence of Pico/Nano Satellites for Atmospheric Research and Technology Testing, AIAA Progress Series in Astronautics and Aeronautics, Thakker, P. and Shiroma, W. A., ed., Reston, VA: AIAA, 2010.

34. http://www.microchip.com/wwwproducts/Devices.aspx?dDocName=en532303

35. Nomex Website, http://www2.dupont.com/Nomex/en_US/index.html

36. Fujimoto, A., Kikugawa, T., and Lim, T., CubeSat Stackable Interface, EE 496 Report, 1st ed., Univ. of Hawaii, Spring 2008.

37. Fujimoto, A., Axelson, J., and Ishida, K., CubeSat Stackable Interface, EE 496 Report, 2nd ed., Univ. of Hawaii, Fall 2008.

38. http://www.iso.org/iso/iso_catalogue/catalogue_tc/catalogue_detail.htm?csnumber=33422

39. http://www.microchip.com/wwwproducts/Devices.aspx?dDocName=en532303

40. http://ww1.microchip.com/downloads/en/DeviceDoc/70291E.pdf

41. http://focus.ti.com/docs/prod/folders/print/tca9539.html#technicaldocuments

42. http://focus.ti.com/docs/prod/folders/print/sn65hvd233.html#technicaldocuments

43. http://www.microchip.com/wwwproducts/Devices.aspx?dDocName=en549421

44. http://ww1.microchip.com/downloads/en/DeviceDoc/S71327_04.pdf

45. http://www.cubesat.org/images/LaunchProviders/mkIII/p-pod%20mk%20iii%20icd.pdf

46. Pumpkin CubeSat Kit website, http://www.cubesatkit.com

47. Akagi, J. M., Tamashiro, T. N., Iwami, R. T., Cardenas, J. M., Akagi, J. T., and Shiroma, W. A., "CubeSat-Based Disaster Detection and Monitoring Systems," in Proceedings of the 6th Responsive Space Conference, Los Angeles, CA, April 2008.

48. Mironer, A. and Regan, F., "Venting of Space-Shuttle Pay Loads," AIAA paper 83-2600, October-November 1983, http://www.accessforeducation.org/docs_ref/AIAAPaper83-2600VentingofSTS Payloads.pdf

49. Furumo, J. "7.UH-NS6-STR401.3JF-Assembly Procedure", Ho'oponopono internal document.

50. "Launch Services Program Level Poly Picosatellite Orbital Deployer (PPOD) and CubeSat Requirements Document," NASA, 2009.

51. "GEVS-SE-RevA, General Environmental Verification Specification for STS and ELV," NASA, Goddard Space Flight Center, June 1996.

52. "Engineering Team Wins Third Place in National Nanosatellite Competition," University of Hawaii News Website, February 25, 2011. http://www.hawaii.edu/news/article.php?aId=4204

53. "Nanosat-6 Flight Competition Review Winners Announced and Nanosat-7 Competition Begins," Wright-Patterson Air Force Base Website, January 24, 2011, http://www.wpafb.af.mil/news/ story.asp?id=123239557

54. "NASA Announces Candidates For CubeSat Space Missions," NASA Website, February 08, 2011, http://www.nasa.gov/home/hqnews/2011/feb/HQ_11-038_CubeSat.html

55. Skrobot, Garrett, NASA Launch Services Program, "ELaNa – Educational Launch of Nanosatellite (ELaNa) Project Status," presented at the 8th Annual CubeSat Developers' Workshop, San Luis Obispo, CA, April 21, 2011. http:// mediasite01.ceng.calpoly.edu/Mediasite/SilverlightPlayer/Default.aspx?peid=f730c55d33a44ac0bb80141d533b665e1d

56. Shiroma, W. A., Akagi, J. M., Wolfe, B., Akagi, J. T., Lee-Ho, Z. and Ohta, A. T. "Big Potential for Small-Satellite Students," 23rd Annual AIAA/Utah State University Conference on Small Satellites, Logan, UT, paper SSC09-XII-7, August 2009.

57. Akagi, J. M., Tamashiro, T. N., Tonaki, W. G. and Shiroma, W. A., "Small Satellites 101: University of Hawaii Small-Satellite Program," in The Emergence of Pico/Nano Satellites for Atmospheric Research and Technology Testing, AIAA Progress Series in Astronautics and Aeronautics, Thakker, P. and Shiroma, W. A., ed., Reston, VA: AIAA, 2010.